Metabolism Substrate With Negative Myocardial Uptake of Iodine-123-BMIPP

Takashi Kudoh, Nagara Tamaki, Yasuhiro Magata, Junji Konishi, Ryuji Nohara, Atsushi Iwasaki, Shinji Ono, Yoshiaki Ohtake, Hiroki Sugihara, Hideki Sugihara, Kogo Kuze, Yoshinori Tsujimura and Tadayoshi Miyazaki

Departments of Nuclear Medicine, Third Division of Department of Internal Medicine, Kyoto University, School of Medicine; Hokkaido University, School of Medicine; Division of Cardiology, Kyoto Mitsubishi Hospital; Department of Internal Medicine, Shiga Medical Center for Adult Diseases; Third Division of Department of Internal Medicine, Osaka Medical College; Department of Radiology, Kyoto Prefectural University of Medicine; Department of Internal Medicine, Takashima General Hospital; Division of Cardiology, Kyoto National Hospital; Division of Cardiology, Ootsu City Hospital, Ootsu; and Division of Internal Medicine, Uji Hospital; Japan

Iodine-123-BMIPP is an iodinated methyl-branched-chain fatty acid. Low uptake of BMIPP relative to thallium or other perfusion tracer indicates metabolically damaged but viable myocardium (for example, ischemic but viable myocardium). In some cases, however, negative myocardial uptake of BMIPP is observed. The main purposes of this study were to assess the frequency of such BMIPP findings and to clarify metabolism of such cases by using PET. **Methods:** Among the 1258 patients who underwent BMIPP scintigraphy, 11 patients (0.9%) showed negative myocardial uptake of BMIPP. Under fasting condition, PET using [^{11}C]palmitate, 2-[^{18}F]fluoro-2-deoxy-D-glucose ([^{18}F]FDG) and [^{11}C]acetate was performed in nine of these 11 patients. **Results:** Global myocardial uptake of [^{11}C]palmitate, expressed as the standardized uptake value, was significantly lower in the patients than in control (3.62 ± 0.44 versus 5.49 ± 1.62; $p < 0.01$). However, the early phase clearance rate of [^{11}C]palmitate and oxidative metabolism was not significantly different. In the fasting state, PET studies showed increased FDG accumulation in seven of nine patients (high group) and decreased accumulation in two patients (low group). In the high group patients, glucose metabolism in the fasting state was similar to that in the normal volunteers after glucose loading ($K_{complex}$: 0.050 ± 0.016 versus 0.038 ± 0.015; p = ns). However, low glucose metabolism was noted in the low group patients ($K_{complex}$: 0.007 and 0.005). **Conclusion:** Negative myocardial uptake of BMIPP is occasionally, but not often, observed. Global uptake of [^{11}C]palmitate was decreased in these patient. The majority of these patients showed "metabolic switching" from normal free fatty acid metabolism to abnormally enhanced glucose metabolism in the fasting state. However, some patients showed decreases in both exogenous glucose utilization and free fatty acid uptake in the fasting state.

Key Words: BMIPP; PET; glucose metabolism; oxidative metabolism; free fatty acid metabolism

J Nucl Med 1997; 38:548–553

The normally perfused myocardium utilizes mainly free fatty acids in the fasting state, whereas fatty acid metabolism is depressed during ischemia. Evaluation of free fatty acid metabolism has been performed with PET using [^{11}C]palmitate (*1–7*). Recently, a variety of radioiodinated compounds have been introduced to probe free fatty acid uptake (*8*). Iodine-123-15-(p-iodophenyl)-3-*R*,*S*-methylpentadecanoic acid (BMIPP) is an iodinated analog of pentadecanoic acid. A methyl group has been introduced at the beta carbon to prolong the retention of this compound in the myocardium. BMIPP is transported into the myocardium similarly to [^{11}C]palmitate, but it is not metabolized by the same beta-oxidation pathway as [^{11}C]palmitate and is trapped in the cytosolic lipid pool (*9–13*). This prolonged retention results in good-quality SPECT images. Previous clinical studies showed decreased regional uptake of BMIPP relative to thallium uptake in ischemic but viable myocardium (*14,15*) and in hypertrophic cardiomyopathy (*15–17*). In some cases, however, [^{123}I]BMIPP scintigraphy shows completely negative myocardial uptake. To clarify the mechanism of the negative uptake of BMIPP, myocardial free fatty acid, glucose and oxidative metabolism have been evaluated in a group which exhibits such negative uptake patterns.

MATERIALS AND METHODS

Patients

A total of 1258 patients underwent BMIPP scintigraphy between January of 1990 and July of 1995 at Kyoto University Hospital and collaborating hospitals. Table 1 shows the diagnoses of the patients. Among them, 1247 patients showed excellent myocardial images with definite uptake of BMIPP in the myocardium, whereas 11 patients (about 0.9%) showed no myocardial uptake of BMIPP. One patient died before the PET study and the severe clinical condition of an other patient precluded BMIPP imaging. The remaining nine patients (ranging from 23 to 65 yr of age) were investigated. Table 2 compiles the clinical information for these nine patients at the time of BMIPP scintigraphy.

For control subjects, [^{11}C]acetate PET was performed in eight normal volunteers, [^{11}C]palmitate PET in five normal volunteers

TABLE 1
Clinical Diagnosis of All BMIPP Study Patients

No. of patients	Diagnosis
630	Chronic coronary artery disease (including OMI, AP, VSA, silent ischemia)
210	AMI
19	CLBBB
1	Syndrome X
27	Valver disorder
79	Hypertension
23	Diabetes mellitus
7	Heart failure
113	Hypertrophic cardiomyopathy
33	Dilating cardiomyopathy
116	Others
1258	Total

OMI = old myocardial infarction; AP = angina pectoris; VSA = vasospastic angina; AMI = acute myocardial infarction; CLBBB = complete left bundle branch block.

Received Mar. 1, 1996; revision accepted Jul. 31, 1996.
For correspondence or reprints contact: Takashi Kudoh, 54 Shogoin-Kawahara, Sakyo-ku, Kyoto 606-01, Japan.

TABLE 2
Clinical Information for Nine Patients Exhibiting Negative Myocardial BMIPP Uptake

Case no.	Age (yr)	Sex	Present illness	History of diabetes	Wall motion	^{201}Tl imaging
1	52	F	HCM (septal hypertrophy)	no	Normal wall motion	Normal perfusion
2	38	M	Arrythmia (PAC)	no	Normal wall motion	Normal perfusion
3	52	M	OMI (post CABG)	Slightly high fasting blood sugar, no medication	Inferior wall akinesis	Inferior wall defect at rest
4	44	F	HT, renal failure	no	Normal wall motion	Normal perfusion
5	62	M	HCM (apical hypertrophy)	no	Normal wall motion	Normal perfusion
6	42	M	OMI (post CABG)	no	Anterior wall hypokinesis	Anterior wall defect at rest
7	64	M	AP (ANT)	no	Anterior wall akinesis	Slight reverse redistribution in anterior wall
8	23	M	OMI (post PTCA)	no	Anterior and lateral wall hypokinesis	Anterior wall defect at rest
9	65	M	HT	no	Normal wall motion	Normal perfusion

and [^{18}F]FDG PET in 11 normal volunteers. Each normal volunteer had no past history of cardiac disease or symptoms. Each normal volunteer was investigated after written informed consent was obtained.

BMIPP Preparation

BMIPP was prepared commercially and contained about 111 MBq of carrier-free 15-(*p*-[^{123}I]iodophenyl)-3-*R*,*S*-methylpentadecanoic acid dissolved in 10.5 mg of urso-dexycholic acid.

BMIPP Protocol

After fasting for at least 5 hr, about 111 MBq of BMIPP was injected at rest, and SPECT imaging was performed 15–20 min later. Stress or rest ^{201}Tl imaging was performed in each case on a separate day. BMIPP transaxial images were interpreted by nuclear cardiologists, who were unaware of the clinical or other scintigraphic data of the patients, to determine whether there was definite BMIPP accumulation in the myocardium. The absence of apparent uptake of the tracer in any segment of the myocardium was considered to be negative myocardial uptake. Planar images were also used to confirm the myocardial uptake. Among all 1258 patients with whom the BMIPP protocol was completed, nine patients showed negative myocardial uptake of BMIPP (Fig. 1). ^{201}Tl imaging showed regional hypoperfusion at rest in three patients with prior myocardial infarction, but none of them showed diffuse hypoperfusion in the left ventricular myocardium.

PET Protocol

Each patient underwent [^{11}C]acetate, [^{11}C]palmitate and [^{18}F]FDG PET studies with a whole-body, 15-slice PET scanner (FWHM; 9 mm in transaxial direction, 7 mm in axial direction) after at least 5 hr of fasting. Each patient was in a stable condition without any cardiac events during the BMIPP and PET studies.

After the patient was positioned in the PET scanner using an echocardiogram, a transmission scan was performed for 20 min. After intravenous administration of [^{11}C]acetate (about 500 MBq), serial images of the myocardial tracer uptake were acquired for 20 min (20 frames of 1 min each) (*18*). On another day, [^{11}C]palmitate (about 400 MBq) was injected as an intravenous bolus, and serial images were recorded for 40 min (20 frames of 2 min each) (*19*). Three hours later, [^{18}F]FDG was injected (about 260 MBq) and serial images were acquired for 52 min (8 frames for 30 sec, followed by 12 frames of 4 min each).

During the acetate PET, the blood pressure and heart rate were measured for calculation of the rate-pressure product. The blood sugar, free fatty acid and insulin levels were determined using venous blood samples obtained from a cubital vein at 5, 25 and 50 min after injection of FDG.

Data Analysis

Seventeen square-shaped (12 × 12 mm) regions of interest (ROI) were placed on the left ventricular wall by using three midventricular transaxial images. Segments showing hypokinetic wall motion found in patients with prior myocardial infarction and angina pectoris were excluded by checking with the data from contrast left ventriculography or echocardiography.

Time-activity curves of the myocardium were made to calculate the washout rate constant of [^{11}C]acetate. In each ROI, the washout rate constant of [^{11}C]acetate (K_{mono}), found to correlate closely with regional myocardial oxygen consumption (*20–22*), was calculated by monoexponential curve fitting and averaged (*23*).

Early uptake of palmitate was calculated from the average count of myocardium at 8–12 min. The standardized uptake value (SUV) (*24,25*) of the left ventricular wall, the arterial count achieved from the left atrial count and the heart/blood activity ratio were calculated from the same early image. The equation for SUV is:

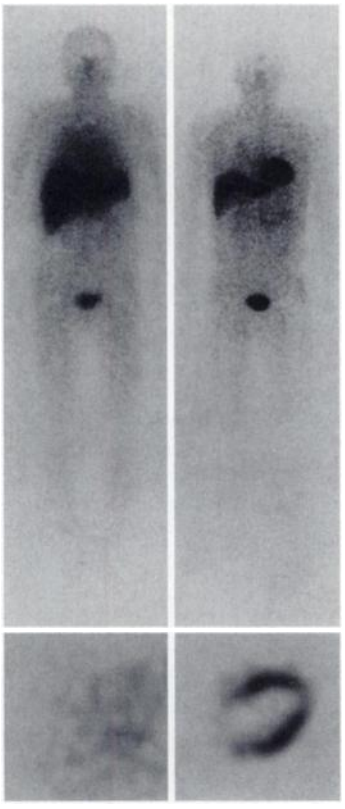

FIGURE 1. BMIPP images. Left: A case of negative myocardial uptake of BMIPP. Right: A normal case. Top row shows whole-body planar image. Bottom row shows a midventricular transaxial SPECT image.

TABLE 3
Uptake and Washout of Carbon-11-Palmitate: Comparison Between Nine Patients and Five Normal Control Subjects*

	n	SUV of myocardium	Blood count	Heart/blood ratio	k of palmitate	$T_{1/2}$ of palmitate
Patients	9	3.62 ± 0.44	2.20 ± 0.24	1.66 ± 0.17	0.030 ± 0.009	25.7 ± 10.3
Controls	5	5.49 ± 1.62	1.60 ± 0.49	3.49 ± 0.66	0.034 ± 0.017	24.9 ± 10.7
p value		<0.01	<0.01	<0.01	ns	ns

*Both patients and control subjects were in the fasting state.

$$SUV = \frac{\text{tissue activity (mCi/g)}}{\text{injected dose (mCi)/body weight (g)}}.$$

Monoexponential curve fitting was performed to calculate the clearance rate constant (k of palmitate) and half time of [^{11}C]palmitate ($T_{1/2}$ of palmitate) in the early phase by the least square fitting technique.

For calculation of the metabolic rate of glucose, a ROI was placed on the left atrium to obtain the arterial time-activity curve. $K_{complex}$ and MRGlc were calculated by Patlak graphical analysis and used as an index of myocardial glucose metabolism (*26*).

Statistical Analysis

Mean values are presented with s.d. For comparison of the patient and control data, the nonpaired Student's t-test was used. Although the data obtained by FDG-PET had two control data (control in the fasting state and after glucose loading), the FDG data were assessed by analysis of variance (ANOVA). When significance was suggested by this analysis, the level of significance was determined using Scheffe's tests. Statistical significance was considered to be present when the p value was less than 0.05.

RESULTS

Frequency and Present History of Negative Myocardial BMIPP Uptake

Negative myocardial uptake of BMIPP was found in 0.87% (11 of 1258) of all the patients who underwent BMIPP scintigraphy. Two cases did not undergo further analysis. Table 2 summarizes the clinical information of the remaining nine cases. There were three cases of old myocardial infarction, one case of angina pectoris, one case of arrhythmia (paroxysmal atrial conduction), two cases of hypertension (one with chronic renal failure) and two cases of hypertrophic cardiomyopathy. Four patients had regional wall motion and perfusion abnormalities. No other clinical symptoms were found. No relationships were found between the present history or past illness and negative myocardial uptake of BMIPP.

Free Fatty Acid Metabolism and Uptake

Each of the patients with negative myocardial uptake of BMIPP showed poor visualization of the myocardium and delayed clearance of [^{11}C]palmitate from the blood (Fig. 2, Table 3). The SUV of the left ventricular wall was significantly lower in the patients with negative myocardial uptake of BMIPP than in the normal control subjects (3.62 ± 0.44 versus 5.49 ± 1.62; $p < 0.01$). Conversely, the arterial count was significantly higher in the patients (2.20 ± 0.24 versus 1.60 ± 0.49; $p < 0.01$). Thus, the heart/blood activity ratio was significantly lower in the cases of negative myocardial uptake of BMIPP (1.66 ± 0.17 versus 3.49 ± 0.66; $p < 0.01$). On the other hand, there was no significant difference in the k of palmitate or the $T_{1/2}$ of palmitate between the patients and the control patients.

Oxidative Metabolism

K_{mono} values, used as an index of myocardial oxidative metabolism, were almost the same as for the normal control subjects (0.060 ± 0.016 versus 0.072 ± 0.020; p = ns). The corrected K_{mono} (K_{mono} value divided by the rate-pressure product) was also similar to that of the normal control subjects (7.51 ± 1.74 versus 8.52 ± 2.97 ($\times 10^{-6}$); p = ns). Rate-pressure product was not different (8387 ± 2311 versus 8808 ± 1831; p = ns)

Glucose Utilization

By visual analysis, the patients were divided into the following two groups according to FDG accumulation in the myocardium in the fasting state: a high group showing high accumulation of FDG, and a low group showing poor FDG accumulation in myocardium in the fasting state (Fig. 3).

The glucose metabolism of the fasting patients was compared with the glucose metabolism of the normal control subjects after glucose loading and in the fasting state (Table 4). $K_{complex}$ in the high group patients in the fasting state tended to be higher but not significantly different from $K_{complex}$ in the normal subjects in the glucose loading, but significantly higher than $K_{complex}$ in the normal subjects in the fasting state (0.050 ± 0.016 versus 0.038 ± 0.015 and 0.007 ± 0.007, $p < 0.01$ between the high group and normal fast, normal load and normal fast). The metabolic rate of glucose (MRGlc) in the high group patients was similar to MRGlc of the normal control subjects under glucose loading, and significantly higher than MRGlc of the normal control subjects in the fasting state (0.34 ± 0.10 versus 0.44 ± 0.13 and 0.05 ± 0.05, $p < 0.01$ between the high group and normal fast, normal load and normal fast). The low group had very low $K_{complex}$ and MRGlc values ($K_{complex}$ = 0.007 and 0.005; MRGlc = 0.06 and 0.06). Due to the small number of patients, statistical analysis was not performed.

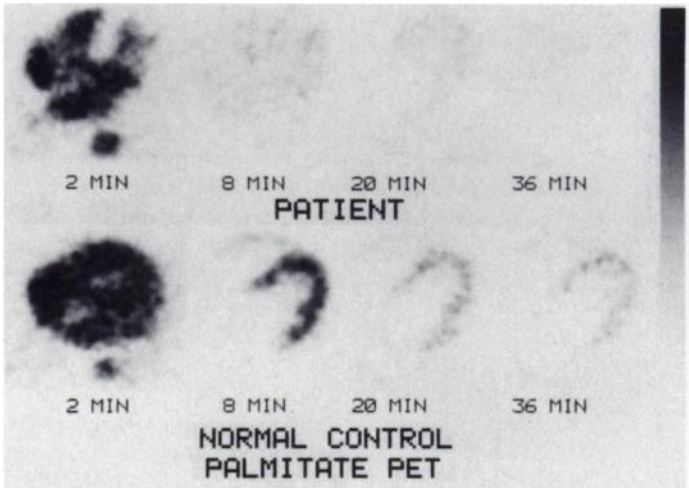

FIGURE 2. Serial [^{11}C]palmitate PET images of Patient 1 (top) and normal control subject (bottom).

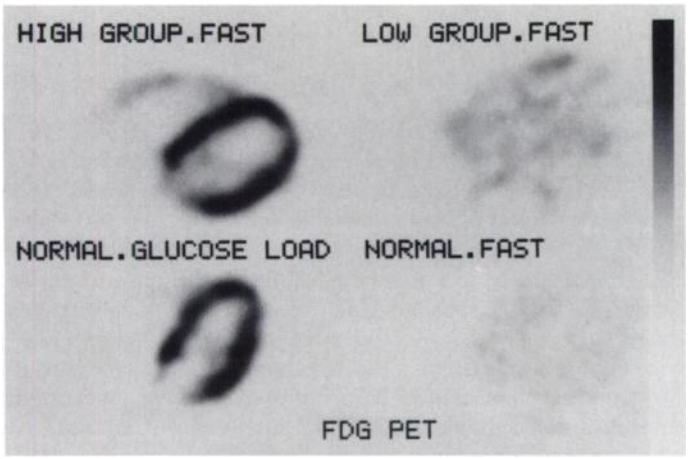

FIGURE 3. FDG images made by summation of 40–52 min after infection of FDG. Top left: Image of the high group obtained in the fasting state. Top right: Image of the low group obtained in the fasting state. Images of normal control subjects are shown in the bottom row for comparison (bottom left = glucose loading state; bottom right = fasting state).

Blood Sugar, Insulin and Free Fatty Acid Levels

To clarify the etiology of this difference in glucose metabolism, the blood sugar, insulin and free fatty acid levels were evaluated (Table 4). The patients in the low group showed an extremely high free fatty acid level in the fasting state.

In the high group, the serum glucose levels and insulin levels were significantly lower than the levels in the normal control subjects under glucose loading, and similar to the levels in the normal control subjects in the fasting state. The free fatty acid levels were similar to the levels in the normal control subjects in the fasting state and tended to be higher than the level in the normal control subjects under glucose loading. However, due to the relatively large s.d., no significant differences were found among the levels in the high group, the normal control subjects in the fasting state and the normal control subjects under glucose loading.

In patients of the low group, the serum pyruvate and lactate level was analyzed. One patient showed relatively high serum pyruvate level (1.70 mg/dl; normal range 0.30–0.94 mg/dl). But the other patient showed normal serum pyruvate level (0.80 mg/dl). Both of two patients of low group showed normal serum lactate level (12.9 and 7.4 mg/dl; normal range 3.3–14.9 mg/dl).

DISCUSSION

This study demonstrated occasional absence of myocardial uptake of BMIPP without any relation to the patient's history of cardiac disease. PET studies indicated abnormal free fatty acid uptake but almost normal myocardial oxidative metabolism. In addition, these cases can be divided into those with enhanced glucose utilization even under fasting conditions (high group) and those without enhanced glucose utilization (low group).

Fatty Acid Uptake and Metabolism

The myocardium utilizes mainly free fatty acids under fasting conditions. BMIPP is modified radioiodinated fatty acid which have prolonged retention suitable for SPECT imaging. Several animal experimental and human studies have shown a discrepancy in the myocardial distribution between BMIPP and flow tracer in the ischemic myocardium (*14,15,27–30*) and the myocardium of hypertrophic cardiomyopathy (*15–17*). Stunned and hibernating myocardium may be associated with such a mismatch between the flow and BMIPP uptake (*14,27,30*).

This study is the first report showing completely negative myocardial uptake of BMIPP under fasting conditions. This negative uptake of BMIPP suggests that free fatty acid metabolism was suppressed throughout the myocardium without any relation to wall motion or perfusion. Myocardial free fatty acid metabolism has been assessed with PET and [^{11}C]palmitate (*1,3,5,7,31*). In the patients with negative myocardial uptake of BMIPP, the clearance of [^{11}C]palmitate from the blood was slow, and the myocardial uptake of [^{11}C]palmitate was significantly lower than in normal subjects (Table 3), indicating suppression of myocardial free fatty acid uptake. However, the washout of [^{11}C]palmitate from the myocardium was not significantly different.

Based on a previous study of beta-oxidation of free fatty acids, the washout curve of [^{11}C]palmitate was analyzed. The low myocardial uptake without abnormal washout indicates a striking decrease in free fatty acid uptake but with a normal beta-oxidation mechanism in the myocardium, where fatty acids are trapped. According to our previous study, myocardial uptake of BMIPP correlated closely with the uptake of [^{11}C]palmitate, but not with the clearance of [^{11}C]palmitate (*32*). Thus, the negative myocardial uptake of BMIPP may reflect only abnormal uptake, not a change in alteration of beta-oxidation.

Alternatively, the very low myocardial uptake of [^{11}C]palmitate may cause a large statistical error in the washout curve analysis. The uptake and oxidation of free fatty acids are not completely separated in the mechanism. The uptake of [^{11}C]palmitate should be influenced by intracellular oxidation. Wyns et al. (*33*) reported a reduced retention fraction with inhibited free fatty acid metabolism. Fox et al. (*34*) showed an increase in back-diffusion of [^{11}C]palmitate in the ischemic myocardium. Thus, decreased uptake of [^{11}C]palmitate may indicate reduced intracellular free fatty acid metabolism.

On BMIPP scintigraphy, the tracer was not seen at all in the myocardium, but high blood pool activity was observed. On [^{11}C]palmitate PET, visualization of the left ventricular wall was very poor but not completely negative in any of the patients. The uptake of long chain fatty acid such as palmitate is a facilitated process and mediated by a fatty acid-binding protein (*35,36*). Similarly, fatty acid-binding proteins may play some role in BMIPP uptake. Some abnormality in this fatty-acid binding protein should be considered. For evaluation of this hypothesis, myocardial wall biopsy is warranted.

One important possible explanation of negative myocardial uptake of BMIPP is back diffusion. The possibility of extremely high back diffusion can't be excluded, because the BMIPP

TABLE 4
Myocardial Glucose Metabolism Evaluated by $K_{complex}$ and MRGlc and Serum Glucose, Insulin and Free Fatty Acid Levels

Subjects	n	$K_{complex}$ (ml/min/g)	MRGlc (μmol/min/g)	Blood sugar (mg/dl)	Insulin (μU/ml)	Free fatty acids (μEq/liter)
Low group	2	0.007, 0.005	0.06, 0.06	102.0, 127.0	13.7, 31.3	1861.6, 2737.0
High group	7	0.050 ± 0.016	0.34 ± 0.10	82.8 ± 8.1	9.6 ± 4.5	793.3 ± 215.8
Control (glucose load)	5	0.038 ± 0.015	0.44 ± 0.13	142.5 ± 17.6	80.9 ± 35.1	296.3 ± 161.7
Control (fasting)	6	0.007 ± 0.007	0.05 ± 0.05	89.3 ± 3.7	15.7 ± 9.7	951.5 ± 630.2

image was not achieved until 15–20 min after injection of BMIPP. Further examination is warranted.

Oxidative Metabolism

This study indicated that oxidative metabolism was not significantly different between the patients with no myocardial uptake of BMIPP and the normal control subjects. The mechanism of decrease in the myocardial uptake of BMIPP in our cases should have no relation with reduction of oxidative metabolism or ATP synthesis. This normal K_{mono} level also suggests that there is no apparent impairment of the myocardial cells.

Glucose Metabolism

We hypothesized that there is a metabolic shift from free fatty acids to glucose under fasting conditions. In seven of the nine cases studied, glucose utilization was enhanced and similar to glucose loading. Enhanced glucose metabolism under fasting conditions is used as a marker of ischemic but viable myocardium (*37,38*). However, in these seven cases, abnormally enhanced glucose metabolism was observed throughout the myocardium without evidence of global myocardial ischemia in the thallium study, or impairment of the left ventricle function. Stunned myocardium may cause a high uptake of FDG (*39*). However, this is excluded due to normokinetic motion. Normal cardiac function and normal oxidative metabolism suggests metabolic switching from free fatty acid metabolism to glucose metabolism. Thus, in the high group patients, carbohydrates may be used as a major energy source at all times, even with low serum glucose and insulin levels in the fasting state.

In the low group patients, however, there was no significant enhancement of [^{18}F]FDG uptake in the myocardium associated with reduced uptake of [^{11}C]palmitate. This indicates that neither exogenous free fatty acids nor glucose was used as the principal myocardial energy source. Since there was no impairment of oxidative metabolism, some substrate must serve as the main energy source of the myocardium. One possible substrate is short-chain fatty acids. El Alaoui-Talibi and Moravec (*40*) showed that the mechanism of free fatty acid transport into the mitochondria is different between palmitate and octanoate. The carnitine transport system is important in palmitate metabolism, but not in octanoate metabolism. Thus, uptake of BMIPP or palmitate may not reflect short-chain fatty acid uptake and metabolism.

Other substrates such as pyruvate, lactate and amino acids may be used as energy sources. In the low group cases, serum pyruvate and lactate levels were examined, one patient showed relatively high serum pyruvate level, but the other patient showed normal serum pyruvate level. Both of the two low group patients showed normal serum lactate level. If these substrates do not show extremely high serum concentration, they cannot produce a sufficient energy supply required to maintain normal cardiac work. Further examination and search for other energy supplies such as amino acids are needed.

In two patients without abnormal enhancement of myocardial glucose utilization, an extremely high level of serum free fatty acids was found. There may be some relation between this abnormally high free fatty acid level and low free fatty acid uptake without enhancement of glucose utilization under fasting conditions. Competitive inhibition between a high level of intrinsic free fatty acids and a very small amount of injected extrinsic free fatty acids ([^{11}C]palmitate) might explain this finding. These two patients also showed a slightly high level of blood sugar and insulin. Interestingly, both of these patients had hypertrophic cardiomyopathy. Metabolic alterations may play some role in the pathophysiological conditions of cardiomyopathy in these patients.

CONCLUSION

Approximately 0.9% of the 1258 patients who underwent BMIPP scintigraphy showed negative myocardial uptake of BMIPP. The PET study suggested a decrease in fatty acid uptake but normal oxidative metabolism in the myocardium of these patients. The patients were subdivided into an abnormally high FDG uptake group under fasting conditions indicating metabolic switching from normal free fatty acid metabolism to abnormally enhanced glucose metabolism, and a low FDG uptake group, indicating that some other substrates were used in these myocardium. These data indicate negative myocardial uptake of BMIPP as a result of alteration of myocardial substrate uptake and utilization.

ACKNOWLEDGMENTS

We thank Eiji Tadamura, Naoya Hattori, Madoka Tateno, Tatsuhiko Hada and Ryohei Hosokawa for assistance with PET studies and Satoshi Sasayama and Toru Fujita and the cyclotron staff for technical assistance. We also thank Nihon Medi-Physics for supplying the BMIPP.

REFERENCES

1. Klein MS, Goldstein RA, Welch MJ, Sobel BE. External assessment of myocardial metabolism with [^{11}C]palmitate in rabbit hearts. *Am J Physiol* 1979;237:H51–H58.
2. Hoffman EJ, Phelps ME, Weiss ES, et al. Transaxial tomographic imaging of canine myocardium with ^{11}C-palmitic acid. *J Nucl Med* 1977;18:57–61.
3. Sobel BE, Weiss ES, Welch MJ, Siegel BATer-Pogossian MM. Detection of remote myocardial infarction in patients with positron emission transaxial tomography and intravenous ^{11}C-palmitate. *Circulation* 1977;55:853–857.
4. Schon HR, Schelbert HR, Robinson G, Najafi A, Huang SC, et al. Carbon-11-labeled palmitic acid for the noninvasive evaluation of regional myocardial fatty acid metabolism with positron-computed tomography. I. Kinetics of ^{11}C palmitic acid in normal myocardium. *Am Heart J* 1982;103:532–547.
5. Schelbert HR, Henze E, Keen R, Schon HR, Hansen H, et al. Carbon-11-palmitate for the noninvasive evaluation of regional myocardial fatty acid metabolism with positron-computed tomography. IV. In vivo evaluation of acute demand-induced ischemia in dogs. *Am Heart J* 1983;106:736–750.
6. Schelbert HR, Henze E, Schon HR, Keen R, Hansen H, et al. Carbon-11-palmitate for the noninvasive evaluation of regional myocardial fatty acid metabolism with positron computed tomography. III. In vivo demonstration of the effects of substrate availability on myocardial metabolism. *Am Heart J* 1983;105:492–504.
7. Schon HR, Schelbert HR, Najafi A, Hansen H, Huang H, et al. Carbon-11-labeled palmitic acid for the noninvasive evaluation of regional myocardial fatty acid metabolism with positron-computed tomography. II. Kinetics of ^{11}C palmitic acid in acutely ischemic myocardium. *Am Heart J* 1982;103:548–561.
8. Knapp FJ, Kropp J. Iodine-123-labeled fatty acids for myocardial SPECT: current status and future perspectives. *Eur J Nucl Med* 1995;22:361–381.
9. Knapp F Jr, Ambrose KR, Goodman MM. New radioiodinated methyl-branched fatty acids for cardiac studies. *Eur J Nucl Med* 1986;12:S39–S44.
10. Ambrose KR, Owen BA, Goodman MM, Knapp F Jr. Evaluation of the metabolism in rat hearts of two new radioiodinated 3-methyl-branched fatty acid myocardial imaging agents. *Eur J Nucl Med* 1987;12:486–491.
11. Yamamichi Y, Kusuoka H, Morishita K, Shirakami Y, Kurami M, et al. Metabolism of iodine-123-BMIPP in perfused rat hearts. *J Nucl Med* 1995;36:1043–1050.
12. Knapp FJ. Myocardial metabolism of radioiodinated BMIPP [Editorial]. *J Nucl Med* 1995;36:1051–1054.
13. Morishita S, Kusuoka H, Yamamichi Y, Suzuki N, Kurami M, et al. Kinetics of radioiodinated species in subcellular fractions from rat hearts following administration of iodine-123-labeled 15-(*p*-iodophenyl)-3-(*R,S*)-methylpentadecanoic acid (BMIPP). *Eur J Nucl Med* 1996;23:383–389.
14. Nishimura T, Uehara T, Strauss HW. Radionuclide assessment of stunned myocardium by alterations in perfusion, metabolism and function. *Jpn Circ J* 1991;55:913–918.
15. Knapp FJ, Franken P, Kropp J. Cardiac SPECT with iodine-123-labeled fatty acids: evaluation of myocardial viability with BMIPP. *J Nucl Med* 1995;36:1022–1030.
16. Kurata C, Tawarahara K, Taguchi T, Aoshima S, Kobayashi A, et al. Myocardial emission computed tomography with iodine-123-labeled beta-methyl-branched fatty acid in patients with hypertrophic cardiomyopathy. *J Nucl Med* 1992;33:6–13.
17. Takeishi Y, Chiba J, Abe S, Tonooka I, Komatani A, et al. Heterogeneous myocardial distribution of iodine-123 15-(*p*-iodophenyl)-3-*R,S*-methylpentadecanoic acid (BMIPP) in patients with hypertrophic cardiomyopathy. *Eur J Nucl Med* 1992;19:775–782.
18. Tamaki N, Magata Y, Takahashi N, Kawamoto M, Torizuka T, et al. Oxidative metabolism in the myocardium in normal subjects during dobutamine infusion. *Eur J Nucl Med* 1993;20:231–237.
19. Tamaki N, Kawamoto M, Takahashi N, Yonekura Y, Magata Y, et al. Assessment of myocardial fatty acid metabolism with positron emission tomography at rest and during dobutamine infusion in patients with coronary artery disease. *Am Heart J* 1993;125:702–710.

20. Brown M, Marshall DR, Sobel BE, Bergmann SR. Delineation of myocardial oxygen utilization with carbon-11-labeled acetate. *Circulation* 1987;76:687–696.
21. Buxton DB, Nienaber CA, Luxen A, Ratib O, Hansen H, et al. Noninvasive quantitation of regional myocardial oxygen consumption in vivo with [1-^{11}C]acetate and dynamic positron emission tomography. *Circulation* 1989;79:134–142.
22. Buxton DB, Schwaiger M, Nguyen A, Phelps ME, Schelbert HR. Radiolabeled acetate as a tracer of myocardial tricarboxylic acid cycle flux. *Circ Res* 1988;63:628–634.
23. Armbrecht JJ, Buxton DB, Brunken RC, Phelps ME, Schelbert HR. Regional myocardial oxygen consumption determined noninvasively in humans with [1-^{11}C]acetate and dynamic positron tomography. *Circulation* 1989;80:863–872.
24. Adler LP, Blair HF, Makley JT, Williams RP, Joyce MJ, et al. Noninvasive grading of musculoskeletal tumors using PET. *J Nucl Med* 1991;32:1508–1512.
25. Haberkorn U, Strauss LG, Dimitrakopoulou A, Engenhart R, Oberdorfer F, et al. PET studies of fluorodeoxyglucose metabolism in patients with recurrent colorectal tumors receiving radiotherapy. *J Nucl Med* 1991;32:1485–1490.
26. Gambhir SS, Schwaiger M, Huang SC, Krivokapich J, Schelbert HR, et al. Simple noninvasive quantification method for measuring myocardial glucose utilization in humans employing positron emission tomography and fluorine-18-deoxyglucose. *J Nucl Med* 1989;30:359–366.
27. Tamaki N, Kawamoto M, Yonekura Y, Fujibayashi Y, Takahashi N, et al. Regional metabolic abnormality in relation to perfusion and wall motion in patients with myocardial infarction: assessment with emission tomography using an iodinated branched fatty acid analog. *J Nucl Med* 1992;33:659–667.
28. Nishimura T, Sago M, Kihara K, Oka H, Shimonagata T, et al. Fatty acid myocardial imaging using ^{123}I-beta-methyl-iodophenyl pentadecanoic acid (BMIPP): comparison of myocardial perfusion and fatty acid utilization in canine myocardial infarction (occlusion and reperfusion model). *Eur J Nucl Med* 1989;15:341–345.
29. De-Geeter F, Franken PR, Knapp F Jr, Bossuyt A. Relationship between blood flow and fatty acid metabolism in subacute myocardial infarction: a study by means of ^{99m}Tc-sestamibi and ^{123}I-beta-methyl-iodo-phenyl pentadecanoic acid. *Eur J Nucl Med* 1994;21:283–291.
30. Franken PR, De-Geeter F, Dendale P, Demoor D, Block P, et al. Abnormal free fatty acid uptake in subacute myocardial infarction after coronary thrombolysis: correlation with wall motion and inotropic reserve. *J Nucl Med* 1994;35:1758–1765.
31. Lerch RA, Bergmann SR, Ambos HD, Welch MJ, Ter-Pogossian MM, et al. Effect of flow-independent reduction of metabolism on regional myocardial clearance of ^{11}C-palmitate. *Circulation* 1982;65:731–738.
32. Kawamoto M, Tamaki N, Yonekura Y, Magata Y, Tadamura E, et al. Significance of myocardial uptake of ^{123}I-labeled beta-methyl iodophenyl pentadecanoic acid: comparison with kinetics of ^{11}C-labeled palmitate in positron emission tomography. *J Nucl Cardiol* 1994;1:522–528.
33. Wyns W, Schwaiger M, Huang SC, Buxton DB, Hansen H, et al. Effects of inhibition of fatty acid oxidation on myocardial kinetics of ^{11}C-labeled palmitate. *Circ Res* 1989;65:1787–1797.
34. Fox KA, Abendschein DR, Ambos HD, Sobel BE, Bergmann SR. Efflux of metabolized and nonmetabolized fatty acid from canine myocardium. Implications for quantifying myocardial metabolism tomographically. *Circ Res* 1985;57:232–243.
35. Samuel D, Paris S, Ailhaud G. Uptake and metabolism of fatty acids and analogues by cultured cardiac cells from chick embryo. *Eur J Biochem* 1976;64:583–595.
36. Gloster J, Harris P. Fatty acid binding to cytoplasmic proteins of myocardium and red and white skeletal muscle in the rat. A possible new role for myoglobin. *Biochem Biophys Res Commun* 1977;74:506–513.
37. Schelbert HR, Henze E, Phelps ME, Kuhl DE. Assessment of regional myocardial ischemia by positron-emission computed tomography. *Am Heart J* 1982;103:588–597.
38. Marshall RC, Tillisch JH, Phelps ME, Huang SC, Carson R, et al. Identification and differentiation of resting myocardial ischemia and infarction in man with positron computed tomography, ^{18}F-labeled fluorodeoxyglucose and ^{13}N-ammonia. *Circulation* 1983;67:766–778.
39. Schwaiger M, Schelbert HR, Ellison D, Hansen H, Yeatman L, et al. Sustained regional abnormalities in cardiac metabolism after transient ischemia in the chronic dog model. *J Am Coll Cardiol* 1985;6:336–347.
40. El Alaoui-Talibi Z, Moravec J. Carnitine transport and exogenous palmitate oxidation in chronically volume-overloaded rat hearts. *Biochim Biophys Acta* 1989;1003:109–114.

Dipyridamole Scintigraphy and Intravascular Ultrasound After Successful Coronary Intervention

Rainald Bachmann, Udo Sechtem, Eberhard Voth, Jörg Schröder, Hans W. Höpp and Harald Schicha
Departments of Nuclear Medicine and Internal Medicine, University of Cologne, Cologne, Germany

Despite angiographically successful interventions, perfusion defects are not uncommonly observed in postinterventional perfusion scintigrams. The aim of this study was to test the hypothesis that perfusion defects after coronary intervention are associated with a significant residual stenosis in the treated vessel segment detectable by intravascular ultrasound but not by angiography. **Methods:** Forty consecutive patients with angiographically successful coronary interventions were prospectively studied by intravascular ultrasound immediately after the intervention. Within 48 hr after the intervention all patients had myocardial scintigraphy using ^{99m}Tc-methoxyisobutyl-isonitrile SPECT after dipyridamole stress. Myocardial perfusion defects in the scintigram were assigned to a segmental left ventricular model and compared to the perfusion territory of the treated vessel estimated from the coronary angiogram **Results:** Twenty of 40 patients had reversible myocardial perfusion defects. Mean ultrasound area stenosis was 50% in these patients and 33% in patients without perfusion defects ($p < 0.002$); ultrasound percent plaque area was 75% versus 63% ($p < 0.0001$), respectively. The best concordance between residual area stenosis and perfusion defects was found for an ultrasound area stenosis ≥40%. **Conclusion:** Patients with stress-induced myocardial perfusion defects immediately after successful coronary intervention show high-grade residual stenoses that are more pronounced in patients with perfusion defects than in patients with normal postinterventional scintigrams. In addition, vessels serving myocardial regions with perfusion defects showed a significantly higher plaque burden indicating diffuse atherosclerotic changes in the vessel. The evaluation of the postprocedural result by intravascular ultrasound contributes to a better understanding of the discrepancy between the angiographic finding of a widely patent vessel but scintigraphic evidence of impaired perfusion.

Key Words: intravascular ultrasound; coronary intervention; dipyridamole; technetium-99m-MIBI; SPECT

J Nucl Med 1997; 38:553–558

Despite angiographically successful interventions, residual ischemia in the perfusion territory of the treated coronary artery is not uncommonly observed in postinterventional perfusion scintigrams. Reversible perfusion defects have been demonstrated by thallium scintigraphy in up to 40% of the patients after angioplasty (*1–4*). These patients seem to have a higher risk of developing restenosis within the next 6 mo. The pathophysiology underlying such persisting ischemia is not fully understood. Different explanations have been put forward: some authors claim a vascular dysregulation and an impaired coronary flow reserve to be responsible (*5,6*), whereas others suggest an impaired uptake of the radiotracer due to persisting metabolic abnormalities in the dependent left ventricular region (*2,7*). Still others suppose that abnormal thallium results after coronary intervention are due to inadequate dilatation of the target vessel or associated lesions (*8*).

Intravascular ultrasound is a relatively new method with the capability to clearly delineate the structure of the arterial wall and the extent of atherosclerotic plaque, allowing a more

Received Mar. 22, 1996; revision accepted Aug. 2, 1996.
For correspondence or reprints contact: Udo Sechtem, MD, Klinik III für Innere Medizin, Universität zu Köln, Joseph-Stelzmann-Str. 9, D-50924 Köln, Germany.